PERIOD TRIPLING STATES AND NON-MONOTONIC ENERGY DISSIPATION IN COUPLED MEMS RESONATORS

Mingkang Wang[1,2], Diego J. Perez-Morelo[1,2], Daniel Lopez[3,1], and Vladimir A. Aksyuk[1]
[1]Microsystems and Nanotechnology Division, National Institute of Standards and Technology, Gaithersburg, MD 20899 USA
[2]Institute for Research in Electronics and Applied Physics, University of Maryland, College Park, MD 20742, USA
[3]Materials Research Institute, Penn State University, University Park, PA 16802, USA

ABSTRACT

When two eigenmodes are at internal resonance (IR), i.e. they have commensurate eigenfrequencies, their coupling strength can be significantly enhanced. Rich nonlinear dynamics have been shown at IR. In this work, we present a novel non-monotonic energy dissipation rate of microelectromechanical systems (MEMs) at IR. We demonstrate that the MEMs can selectively dissipate via two largely distinctive pathways, solely depending on the choice of their relative initial phase. Remarkably, these novel and complicated behaviors can be modeled by an intuitive parametric-oscillator-like model. Our work illuminates a path to dissipation engineering, frequency stabilization, and sensitivity enhancement.

KEYWORDS

Dissipation, internal resonance, non-monotonic energy dissipation rate, period-tripling states

INTRODUCTION

Understanding energy dissipation is critical both for fundamental science and practical applications, such as for quantum information [1,2] and fundamental timing and sensing applications [3–5]. A fundamental picture of energy dissipation is that a non-equilibrium harmonic oscillator exponentially losses energy to a thermal bath. Based on this basic picture, many efforts are made to engineer the dissipation rate by either modifying the coupling strength with the thermal bath, such as via phononic bandgap structures [6], or introducing an extra coupling source, i.e. another bath - another oscillator [7–9]. Dissipation engineering has very different goals, for example, a switch demands a high energy dissipation rate for a short transition time [10,11], while more commonly, a low dissipation rate is desired for good isolation of oscillators from the environment which is a benefit for many scenarios, such as extending coherence time of quantum computer [12–14], reducing thermal noise for sensing and timing purposes, and reducing power consumption. In particular, a selective dissipation rate without disturbing other parameters of the system could be a good compromise for the different needs.

Internal resonance (IR) [15] is a competent candidate for dissipation engineering via mode coupling. Different from the commonly used parametric coupling of two modes with arbitrary eigenfrequency relationships [16,17], IR happens only when their frequencies have a commensurate relationship (e.g. 1:3), and therefore, has stronger coupling [18]. Recently, IR is intensively studied in the nano/micro-electro-mechanical systems (N/MEMs) and shows rich nonlinear dynamics, such as period-tripling states [19,20], and frequency stabilization in a nonlinear oscillator [21]. Regarding the dissipation at IR, previous works observed anomalous decay rates during the free ringdown of the coupled system. Due to the rapid energy exchange between the modes at IR, one mode in the free ringdown system could present either a faster [8] or slower [7] dissipation rate depending on the system parameter. However, due to the limitation of the setup, only one mode of the system was controllable and measurable, largely limiting the understanding of these novel behaviors. Moreover, recent theoretical research [22] points out that by choosing proper initial conditions of the two modes, even richer nonlinear dynamics could show up, such as the non-monotonic amplitude dependence of decay rate and phase-dependent dissipation paths.

Here we experimentally demonstrate a selective non-monotonic dissipation rate of a double-clamped beam at internal resonance. The two modes under investigation are two eigenmodes of the beam with nearly commensurate eigenfrequencies (1:3) and strong Duffing nonlinearity. By preparing two modes at specific initial conditions, then releasing them and recording their free ringdown simultaneously, we observe that they either lock at internal resonance or bypass it during ringdown. Such selection can be controlled by tuning their initial relative phase before ringdown. If they lock, the high-frequency mode (mode 2) performs as a period-3 parametric drive to the low-frequency mode (mode 1). It creates a period-tripling state, which resembles the period-doubling states for parametric resonators [23]. Under such states, mode 2 transfers energy to mode 1, making it experience an energy gain while the system still loses energy continuously. Finally, when mode 2's energy is lower than the parametric drive threshold, the two modes unlock and dissipate with their intrinsic energy loss. Remarkably, the locked state can last several times longer than the intrinsic dissipation time of mode 1 and of the system. During this process, mode 1 exhibits a non-monotonic dissipation rate as a function of the system energy. If they bypass at internal resonance, we observe a reverse effect, i.e. mode 1 transfers energy to mode 2 and shows a transient faster dissipation rate. For the two cases, the coupled-mode system shows distinct system dissipation rates since the induvial intrinsic dissipation rates of the two modes are different. This locking and bypass dissipation trajectories and the modes' behaviors during locking can be well described by an intuitive period-tripling model where mode 2 acts as a parametric drive to mode 1. This switchable and non-monotonic dissipation rate induced by strong modal coupling could shed light on extending the coherence time and improving frequency stabilization of general resonators used in sensing and timing applications.

SYSTEM AND MEASUREMENT

As shown in Fig. 1(a), the system under investigation is a clamped-clamped beam with two side gates for driving the system and performing an electrical measurement. A laser vibrometer performs optical measurement, simultaneously. The device is placed in a vacuum chamber with pressure $< 1 \times 10^{-5}$ Torr. The lowest order in-plane mode (mode 1) and torsional mode (mode 2) shown in Fig. 1(b) are of eigenfrequencies $\omega_1/2\pi \approx 64.6$ kHz and $\omega_2/2\pi \approx 199.9$ kHz, respectively, with nearly commensurate relationship ($\omega_1 \approx \omega_2/3$). Their intrinsic dissipation rates without coupling are significantly different with the measured value of $\Gamma_1/2\pi \approx 1.5$ Hz and $\Gamma_2/2\pi \approx 3.3$ Hz, respectively.

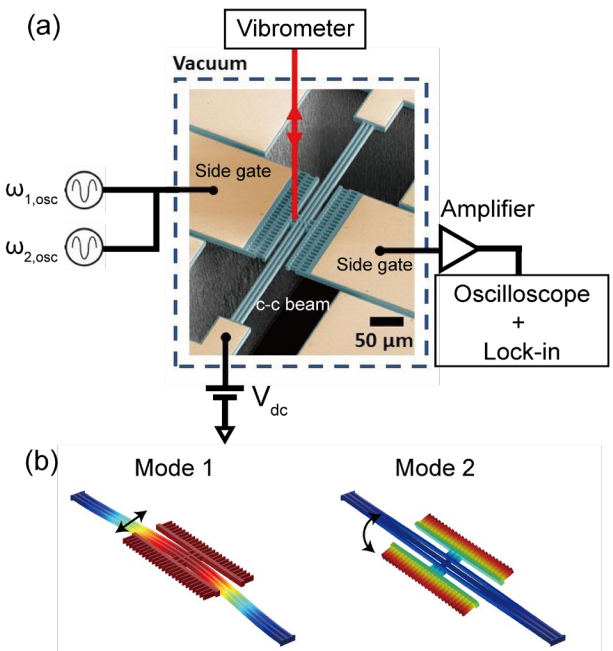

Figure 1: (a) Measurement schematics and false-colored SEM micrograph of the clamp-clamp (c-c) beam MEMS. Optical and electrical measurements are performed, simultaneously. (b) Simulated mode shape of the two coupled modes.

For characterization, the two modes are driven separately, responding with oscillating frequencies $\omega_{1,osc}$ and $\omega_{2,osc}$. When the driving force is strong, mode 1 shows the spring hardening effect while mode 2 presents the softening effects, shown as the orange and green dots in Figure 2, respectively. The *x*-axis of mode 2 (green) is scaled by a factor of three ($\omega_{2,osc}/3$) to compare with mode 1. Here the two modes are driven separately, i.e. when one mode is driven, the other one remains mostly at thermal equilibrium with the bath. The dip on mode1's spectrum (orange) corresponds to the IR frequency of $\omega_{1,osc} = \omega_2/3$ where the model coupling is the strongest, resulting in some energy transfer to mode 2 from mode 1 [24].

In the ringdown experiment, we drive the two modes separately to their initial amplitude $A_{1,0}$ and $A_{2,0}$, labeled as red dots. At time $t = 0$, we turn off their drive simultaneously to let them freely decay. Following their Duffing backbone (black arrows in Figure 2), their frequencies shift due to the exponentially decaying amplitude (Fig. 3) and reach the IR when their oscillating frequency $\omega_{1,osc} = \omega_{2,osc}/3$ (black dots in Figure 2). Since mode 2's softening effect, the IR frequency during ringdown (black dot) is somewhere between the initial frequency of mode 2 (red dot) and the eigenfrequency of mode 2 (black dashed line).

NON-MONOTONIC ENERGY DISSIPATION RATE

At IR, the two modes either lock or bypass each other depending on the initial relative phase. Figure 3(a) and 3(b) presents the frequency and energy of the two modes for the locking case. Before entering IR, the two modes exponentially decay (Fig. 3b) with their intrinsic dissipation rates. Following their Duffing backbone, $\omega_{1,osc}$ decreases while $\omega_{2,osc}$ increases (Fig. 3a) shown as the black arrows in Fig. 2. After entering the locked states, $\omega_{1,osc}$ locks to $\omega_{2,osc}$ and oscillates around it, while $\omega_{2,osc}$ is not largely affected by mode 1. It can be explained considering the situation where mode 2's energy is much larger than mode 1. Only when the two modes are nearly unlocked, mode 1 and mode 2's energies are comparable, and the two modes both present oscillations.

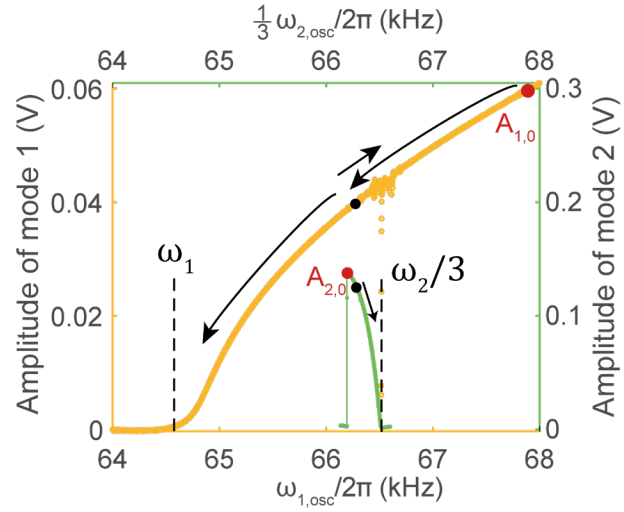

Figure 2. Spectrums of mode1 and mode2 are labeled by yellow and green dots. The oscillating frequency of mode2 is divided by 3. The two modes have opposite Duffing coefficients. In ringdown experiments, we set the initial conditions at $A_{1,0}$ and $A_{2,0}$ (red dots), respectively, and turn off the drive simultaneously. They evolve to equilibrium following the black arrows. After being locked at the internal resonance, the black dots, Mode1 experiences frequency and amplitude increase shown as the short black arrow.

The complete equation of motion for this coupled-mode system is written as:

$$\ddot{q}_1 + \Gamma_1\dot{q}_1 + \omega_1^2 q_1 + \alpha_1 q_1^3 + 3g_{12}q_1^2 q_2 = 0 \quad (1)$$

$$\ddot{q}_2 + \Gamma_2\dot{q}_2 + \omega_2^2 q_2 + \alpha_2 q_2^3 + g_{21}q_1^3 = 0 \quad (2)$$

where q_1 and q_2 are the modal displacement, α_1 and α_2 are the Duffingg coefficients with opposite signs, and g_{12} and g_{21} are the coupling rate. As $q_2 \gg q_1$, Eq. (2) can be simplified to a Duffing oscillator while Eq. (1) can be rewritten as:

$$\ddot{q}_1 + \Gamma_1\dot{q}_1 + \omega_1^2 q_1 + \alpha_1 q_1^3 = q_1^2 F_2(t)\cos[\Phi_2(t)] \quad (3)$$

where the interaction term in Eq. (1) is regarded as a parametric drive with time-varying frequency $\omega_2(t) = \dot{\Phi}_2(t)$ and amplitude $F_2(t)$. Eq. (3) depicts a parametric oscillator under a period-three drive, i.e. $\omega_2(t)/3 = \omega_1(t)$. Similar to parametric oscillators under period-two drive, the period-three drive creates period-tripling states [25,26] that are degenerate with $2\pi/3$ relative phase difference.

During locking, mode 2's eigenfrequency continuously shifts to a higher frequency, pulling Mode 1 to a higher frequency and higher amplitude on its Duffing backbone (short arrow in Fig. 2). As a result, mode 1 shows an anomalous negative dissipation rate (energy gain), as shown in the inset of Fig. 3(b), while the system continuously loses energy. At the end of the locking state, mode 2 is not able to provide enough parametric drive to mode 1, therefore, the two modes unlock from each other, and dissipate again following their own intrinsic dissipate rate. The locking state length, or coherent time, depends on the initial energy of the system. Remarkably, the locking state can last up to ≈ 0.26 s which is around 3 times of the intrinsic dissipation time of mode 1 ($1/\Gamma_1 \approx$ 0.10 s) and 5 times of the system dissipation time ($1/\Gamma_2 \approx$ 0.05 s).

The dynamics of the system can be fully modeled by the Eq. (1-2). However, here we only focus on its long-term evolution (~$1/\Gamma$) and ignore the time-averaged interaction energy. Under such

assumptions, intuitively, the energy loss by mode 2 equals the energy gain by mode 1 after excluding their intrinsic losses:

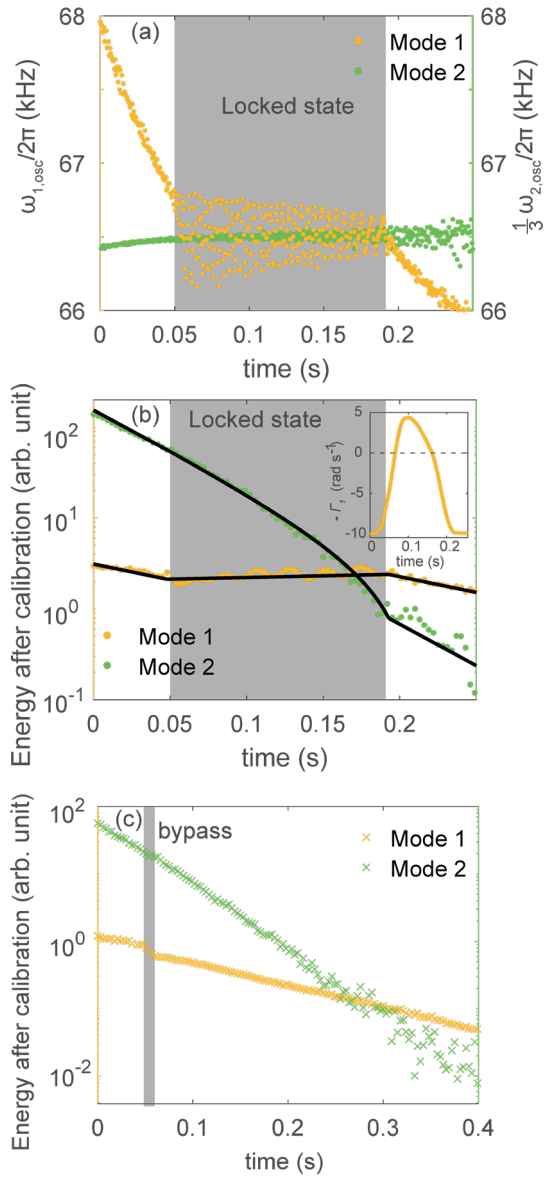

Figure 3. Oscillating frequencies and energy of the two locked modes are presented in (a) and (b), respectively. The yellow and green dots correspond to mode1 and mode2, respectively. The inset of (b) shows the measured relative energy change rate (effective $-\Gamma_1$), illustrating non-monotonic and negative dissipation rate (energy gain) during locking. The bypass case is shown in (c). A rapid energy loss is observed for mode 1 at internal resonance, colored gray.

$$\frac{dE_1}{dt} = -\Gamma_1 E_1 + P \quad (4)$$

$$\frac{dE_2}{dt} = -\Gamma_2 E_2 - P \quad (5)$$

where $E_1 \propto q_1^2$ and $E_2 \propto q_2^2$ are the energy of mode 1 and mode 2, P is the energy exchange rate. As mode 1 amplitude is nearly a constant, $P \approx \Gamma_1 E_1$ can be considered a constant. The black lines in Fig. 3(b) shows the fitted E_1 and E_2 with only one fitting parameter P.

For the bypass case, except for a short rapid energy decay of mode 1 at the IR (gray area in Fig. 3(c)), the two modes continuously exponentially decay with their intrinsic loss rates. The lock or bypass depends on the relative phase between the two modes at the initial state. We can select the dissipation path of the system by setting their initial phase.

Intuitively, the lock or bypass is decided by the energy transfer direction at IR. The direction is governed by their relative phase. For example, if mode 2's phase $\varphi_2/3$ is ahead compared to φ_1, the energy flows from mode 2 to mode 1 and pumps mode 1. Their oscillating frequencies can be maintained at IR although both slowly increase. On the contrary, if mode 1's phase leads, it transfers energy to mode 2 at IR which makes their frequencies bypass IR quickly.

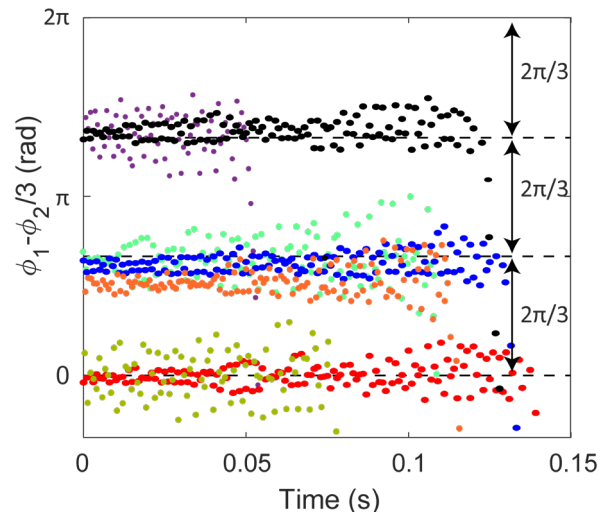

Figure 4. Relative phase of mode1 (φ_1) and mode2 (φ_2) in 7 repeating experiments. φ_1- $\varphi_2/3$ exhibits discrete values of (0, 4π/3, 2π) at period tripling states.

To demonstrate the period-tripling model, we repeat the same ringdown experiment, and we find the system exhibits phase-locking with discrete relative phase φ_1- $\varphi_2/3$ = n×2π/3 shown in Figure 4 where n is an integer. It is consistent with the period-tripling interpretation. The discrete relative phase resembles the n×2π/2 period-doubling states for parametric oscillators.

SUMMARY

In conclusion, we have demonstrated selective energy dissipation pathways of a coupled system at the internal resonance (i.e. two modes with 1:3 commiserate eigenfrequencies). By setting the relative initial phase between the two coupled modes, the two modes can either enter the designated phase-locking state or bypass it during their free ringdown. In the phase-locking path, the coupling from the high-frequency mode (mode 2) acts as a period-three parametric drive to the low-frequency mode (mode 1), locking the phase and making φ_1- $\varphi_2/3$ nearly constant. During the phase-locking, the frequency of the two modes varies with their decaying amplitude along with their Duffing amplitude-frequency relationship while maintaining the 1:3 internal resonance relationship. Since the two modes have opposite Duffing coefficients and mode 2's energy is much larger than mode 1, "slave" mode 1 exhibits a frequency increase together with "master" mode 2, resulting in an energy gain during the locking. It makes mode 1 presents an anomalous non-monotonic energy dissipation rate during the ringdown. Remarkably, the locking time can be

nearly 6 times longer than the system dissipation time scale $1/\Gamma_2$ and 3 times longer than the intrinsic dissipation time scale $1/\Gamma_1$ of mode 1 itself. The findings of phase-locking states and selective dissipation rates are useful for energy dissipation engineerings, such as for fast switches or low-dissipation timing/sensing devices. The proposed intuitive period-tripling model provides a picture to understand the complicated dynamics in coupled nonlinear resonators.

ACKNOWLEDGEMENTS

We thank Dr. Steven Shaw, Dr. Ori Shoshani and Dr. David A. Czaplewski for useful discussions. We thank Dr. Jason J. Gorman, Dr. Damián H. Zanette, Dr. J. Alexander Liddle, and Dr. Marcelo Davanco for reviewing this paper and giving meaningful suggestions. M.W. and D.J.P. are supported by the Cooperative Research Agreement between the University of Maryland and the National Institute of Standards and Technology Center for Nanoscale Science and Technology, Award 70NANB14H209, through the University of Maryland.

REFERENCES

[1] F. Verstraete, M. M. Wolf, and J. Ignacio Cirac, *Quantum Computation and Quantum-State Engineering Driven by Dissipation*, Nature Physics **5**, 9 (2009).

[2] M. Steffen, S. Kumar, D. P. DiVincenzo, J. R. Rozen, G. A. Keefe, M. B. Rothwell, and M. B. Ketchen, *High-Coherence Hybrid Superconducting Qubit*, Phys. Rev. Lett. **105**, 100502 (2010).

[3] X. Liu, J. F. Vignola, H. J. Simpson, B. R. Lemon, B. H. Houston, and D. M. Photiadis, *A Loss Mechanism Study of a Very High Q Silicon Micromechanical Oscillator*, Journal of Applied Physics **97**, 023524 (2004).

[4] M. Li, H. X. Tang, and M. L. Roukes, *Ultra-Sensitive NEMS-Based Cantilevers for Sensing, Scanned Probe and Very High-Frequency Applications*, Nature Nanotechnology **2**, 2 (2007).

[5] M. Weinberg, R. Candler, S. Chandorkar, J. Varsanik, T. Kenny, and A. Duwel1, *Energy Loss in MEMS Resonators and the Impact on Inertial and RF Devices*, in *TRANSDUCERS 2009 - 2009 International Solid-State Sensors, Actuators and Microsystems Conference* (2009), pp. 688–695.

[6] Y. Tsaturyan, A. Barg, E. S. Polzik, and A. Schliesser, *Ultracoherent Nanomechanical Resonators via Soft Clamping and Dissipation Dilution*, Nature Nanotechnology **12**, 776 (2017).

[7] C. Chen, D. H. Zanette, D. A. Czaplewski, S. Shaw, and D. López, *Direct Observation of Coherent Energy Transfer in Nonlinear Micromechanical Oscillators*, Nat Commun **8**, 15523 (2017).

[8] J. Güttinger, A. Noury, P. Weber, A. M. Eriksson, C. Lagoin, J. Moser, C. Eichler, A. Wallraff, A. Isacsson, and A. Bachtold, *Energy-Dependent Path of Dissipation in Nanomechanical Resonators*, Nature Nanotech **12**, 631 (2017).

[9] X. Dong, M. I. Dykman, and H. B. Chan, *Strong Negative Nonlinear Friction from Induced Two-Phonon Processes in Vibrational Systems*, Nature Communications **9**, 1 (2018).

[10] A. F. Vakakis, O. V. Gendelman, L. A. Bergman, D. M. McFarland, G. Kerschen, and Y. S. Lee, *Nonlinear Targeted Energy Transfer in Mechanical and Structural Systems* (Springer Science & Business Media, 2008).

[11] H. Okamoto, I. Mahboob, K. Onomitsu, and H. Yamaguchi, *Rapid Switching in High-Q Mechanical Resonators*, Appl. Phys. Lett. **105**, 083114 (2014).

[12] C. Langer, R. Ozeri, J. D. Jost, J. Chiaverini, B. DeMarco, A. Ben-Kish, R. B. Blakestad, J. Britton, D. B. Hume, W. M. Itano, D. Leibfried, R. Reichle, T. Rosenband, T. Schaetz, P. O. Schmidt, and D. J. Wineland, *Long-Lived Qubit Memory Using Atomic Ions*, Phys. Rev. Lett. **95**, 060502 (2005).

[13] M. Stern, G. Catelani, Y. Kubo, C. Grezes, A. Bienfait, D. Vion, D. Esteve, and P. Bertet, *Flux Qubits with Long Coherence Times for Hybrid Quantum Circuits*, Phys. Rev. Lett. **113**, 123601 (2014).

[14] Y. Wang, M. Um, J. Zhang, S. An, M. Lyu, J.-N. Zhang, L.-M. Duan, D. Yum, and K. Kim, *Single-Qubit Quantum Memory Exceeding Ten-Minute Coherence Time*, Nature Photonics **11**, 10 (2017).

[15] L. Manevitch and A. I. Manevich, *The Mechanics Of Nonlinear Systems With Internal Resonances* (World Scientific, 2005).

[16] J. D. Teufel, T. Donner, D. Li, J. W. Harlow, M. S. Allman, K. Cicak, A. J. Sirois, J. D. Whittaker, K. W. Lehnert, and R. W. Simmonds, *Sideband Cooling of Micromechanical Motion to the Quantum Ground State*, Nature **475**, 359 (2011).

[17] I. Mahboob, K. Nishiguchi, H. Okamoto, and H. Yamaguchi, *Phonon-Cavity Electromechanics*, Nature Physics **8**, 5 (2012).

[18] A. H. Nayfeh and D. T. Mook, *Nonlinear Oscillations* (John Wiley & Sons, 2008).

[19] N. Lörch, Y. Zhang, C. Bruder, and M. I. Dykman, *Quantum State Preparation for Coupled Period Tripling Oscillators*, Phys. Rev. Research **1**, 023023 (2019).

[20] J. Gosner, B. Kubala, and J. Ankerhold, *Relaxation Dynamics and Dissipative Phase Transition in Quantum Oscillators with Period Tripling*, Phys. Rev. B **101**, 054501 (2020).

[21] D. Antonio, D. H. Zanette, and D. López, *Frequency Stabilization in Nonlinear Micromechanical Oscillators*, Nat Commun **3**, 1 (2012).

[22] O. Shoshani, S. W. Shaw, and M. I. Dykman, *Anomalous Decay of Nanomechanical Modes Going Through Nonlinear Resonance*, Sci Rep **7**, 18091 (2017).

[23] H. B. Chan and C. Stambaugh, *Activation Barrier Scaling and Crossover for Noise-Induced Switching in Micromechanical Parametric Oscillators*, Physical Review Letters **99**, (2007).

[24] S. Houri, D. Hatanaka, M. Asano, R. Ohta, and H. Yamaguchi, *Limit Cycles and Bifurcations in a Nonlinear MEMS Resonator with a 1:3 Internal Resonance*, Appl. Phys. Lett. **114**, 103103 (2019).

[25] J. Gosner, B. Kubala, and J. Ankerhold, *Relaxation Dynamics and Dissipative Phase Transition in Quantum Oscillators with Period Tripling*, Phys. Rev. B **101**, 054501 (2020).

[26] Y. Zhang and M. I. Dykman, *Nonlocal Random Walk over Floquet States of a Dissipative Nonlinear Oscillator*, Phys. Rev. E **100**, 052148 (2019).

CONTACT

*V. Aksyuk, tel: +1-301-975-2867; vladimir.aksyuk@nist.gov